Endohedral Clusters

DOI: 10.1002/anie.200604198

Towards a 32-Electron Principle: $Pu@Pb_{12}$ and Related Systems**

*Jean-Pierre Dognon, Carine Clavaguéra, and Pekka Pyykkö**

The 18-electron principle goes back to Langmuir.[1] Its history and interpretation were the subject of a recent paper.[2] Formally it corresponds to fully occupying the *n*s, *n*p, and $(n-1)$d orbitals at a central atom. In fact, the kinetic-energy separation of the ligand orbitals, because of their nodal structures, demands that all 18 states are occupied, even if the metal *n*p (or *n*s) character happens to be negligible.

For early 5f elements the f shell becomes chemically available and remains so until about Am. Theoretically, it could be filled with 14 further electrons to bring the total to 32, a theoretical possibility already evoked by Langmuir.[1] How far towards that limit can one go? Thorocene, $[Th(C_8H_8)_2]$, was classified as a 20-electron case.[2] In metalloactinyl compounds such as linear $[IrThIr]^{2-}$, one could potentially reach 24 electrons.[3] We have now found that the 6p valence band of the recently discovered icosahedral $[Pb_{12}]^{2-}$ shell forms a perfect partner for the 5f shell of an enclosed actinide atom such as plutonium. Detailed DFT calculations suggest that the system is viable. It could, on good grounds, be characterized as a 32e system.

The corresponding empty icosahedral Zintl ions, such as plumbaspherene $[Pb_{12}]^{2-}$ and stannaspherene $[Sn_{12}]^{2-}$, were recently characterized by photoelectron spectroscopy and quantum chemical calculations.[4,5] Characteristic for these ions is that the valence *n*p band is clearly separated from the valence *n*s band. They also afford a new class of endohedral compounds, such as the icosahedral $[M@Pb_{12}]^x$ ($x = +1, 0, -1, -2$; M = Al, Pt, Ni, Pd, Co, among others), studied experimentally by mass spectrometry, ^{207}Pb NMR spectroscopy, and X-ray analysis.[6–9] Density functional calculations were also reported.[6,10,11] In all these studies, the clusters proved to be very stable, and they thus open a branch of novel, chemically inert cluster compounds. Some endohedral gas-phase stannaspherene anions were recently reported.[12]

The relevant electron counts are clarified in Table 1. We here count as magic numbers for icosahedral systems the values *N* [Eq. (1)].

$$N = \sum_{l=0}^{L} 2(2l+1) = 2(L+1)^2 \qquad (1)$$

Table 1: Magic electron numbers *N*, their relation to filling of atomic-type shells, examples of false magic numbers N_{false}, and intermediate magic numbers N_{interm}.[a]

Number	Value	Atomic shell	Γ	Examples
N	2	s	a_g	–
	8	sp	$a_g \oplus t_{1u}$	–
	18	spd	$a_g \oplus t_{1u} \oplus h_g$	WAu_{12}[21]
	32	spdf	$a_g \oplus t_{1u} \oplus h_g \oplus g_u \oplus t_{2u}$[b]	$Pu@Pb_{12}$[c]
	50	spdfg	$a_g \oplus t_{1u} \oplus h_g \oplus g_u \oplus t_{2u} \oplus g_g \oplus h_g$	–
	72	spdfgh	$a_g \oplus t_{1u} \oplus h_g \oplus g_u \oplus t_{2u} \oplus g_g \oplus h_g \oplus t_{1u} \oplus t_{2u} \oplus h_u$	–
N_{false}	50	2s2p2d1f		$[Al@Pb_{12}]^+$[10]
N_{interm}	20	2s1p1d		$Si@Au_{16}$[22]

[a] For chemical examples of centered systems and irreducible representations Γ under group I_h, see reference [13]. [b] In the double group I_h: $a_g \simeq e_{1/2g}$, $t_{1u} \simeq e_{1/2u} \oplus g_{3/2u}$, $t_{2u} \simeq i_{5/2u}$, $g_u \simeq e_{7/2u} \oplus i_{5/2u}$, $h_g \simeq g_{3/2g} \oplus i_{5/2g}$. [c] This work.

Such magic numbers correspond to "spherical aromaticity" in the classification of reference [13]. An earlier example of an empty 32e shell is the theoretically proposed Au_{32} cluster.[14,15] We are not aware of any previous centered 32e cases. The 6p band of $[Pb_{12}]^{2-}$ [10] spans an occupied $a_g \oplus t_{1u} \oplus g_u \oplus h_g$ 26-electron band.

In Table 1 we also point out that multiple occupation of the lower-*l* orbitals can give the same magic number as a single occupation of higher-*l* orbitals. An example of such a *false magic number* is shown for $N = 50$ (note that all 18 states, spanned by $l = 4$, must be "g" while the second spd shell spans $a_g \oplus t_{1u} \oplus h_g$ of I_h). Moreover, depending on details of the radial potential, very stable *intermediate magic numbers* can occur for specific elements. An example is shown for $N = 20$.

Our specific idea is that with a further 6 electrons on top of the 26e plumbaspherene 6p band $a_g \oplus g_u \oplus h_g \oplus t_{1u}$ (HOMO), we obtain a perfect $a_g \oplus g_u \oplus h_g \oplus t_{1u} \oplus t_{2u}$ 32e configuration. The

[*] Prof. Dr. P. Pyykkö
Department of Chemistry
University of Helsinki
P.O. Box 55, 00014 Helsinki (Finland)
Fax: (+358) 9-191-50169
E-mail: Pekka.Pyykko@helsinki.fi
Dr. J.-P. Dognon
Present and permanent address:
CEA/Saclay, DSM/DRECAM/SCM, 91191 Gif-sur-Yvette (France)
Dr. C. Clavaguéra
Present address:
Laboratoire des Mécanismes Réactionnels
Département de Chimie, Ecole Polytechnique, CNRS
91128 Palaiseau Cedex (France)

[**] The Finnish group belongs to the Finnish Centre of Excellence in Computational Molecular Science (2006-2011). The grants 200903 and 266102 from The Academy of Finland are also gratefully acknowledged. C.C. thanks the Magnus Ehrnrooth Foundation for a postdoctoral scholarship. J.P.D. is supported by the French CEA-Direction des Sciences de la Matière/University of Helsinki collaboration. We thank J. P. Desclaux for his help in the use of the MCDFGME program. Considerable computer resources were obtained from CSC Computing, Espoo, Finland and at the "Ametisti" campus cluster.

Supporting information for this article is available on the WWW under http://www.angewandte.org or from the author.

t_{2u} from the actinide 5f band is then added to the count. The additional electrons can come from Pu, for instance.

The calculated molecular geometries and energy gaps are listed in Table 2, and an energy analysis is presented in Table 3. The molecular orbitals of both the empty $[Pb_{12}]^{2-}$ shell and the neutral $Pu@Pb_{12}$ molecule are shown in Figure 1. The orbital-energy spectra for $[Pb_{12}]^{2-}$ and $An@Pb_{12}$ (An = Pu, Am, Cm) are shown in Figure 2 and Figure S1 in the Supporting Information. The densities of states are shown for these four cases in Figure 3. Finally, the electron localization function (ELF) of $Pu@Pb_{12}$ (Figure 4) clearly reveals the radial bonds. The related theoretical methods are outlined in the Supporting Information.

Table 2: Calculated geometric data and the HOMO–LUMO gap for the $[Pb_{12}]^{2-}$ and $[M@Pb_{12}]^{x}$ clusters.

Molecule	Point-group symmetry	r_{M-Pb}[a] [Å]	HOMO–LUMO [eV]
$[Pb_{12}]^{2-}$	I_h	3.14	3.08
$Yb@Pb_{12}$	I_h	3.28	0.80
$[Th@Pb_{12}]^{4-}$	C_5	3.61, 4.52	1.26
$[U@Pb_{12}]^{2-}$	D_{5h}	3.48, 4.05	1.26
$[Np@Pb_{12}]^{-}$[a]	D_{5h}[b]	3.48, 4.15	1.20
$Pu@Pb_{12}$	I_h	3.33	1.93
$[Am@Pb_{12}]^{+}$	I_h	3.35	2.45
$[Cm@Pb_{12}]^{2+}$	I_h	3.37	0.85

[a] r is the distance from the midpoint to the lead atoms. [b] One imaginary frequency remains.

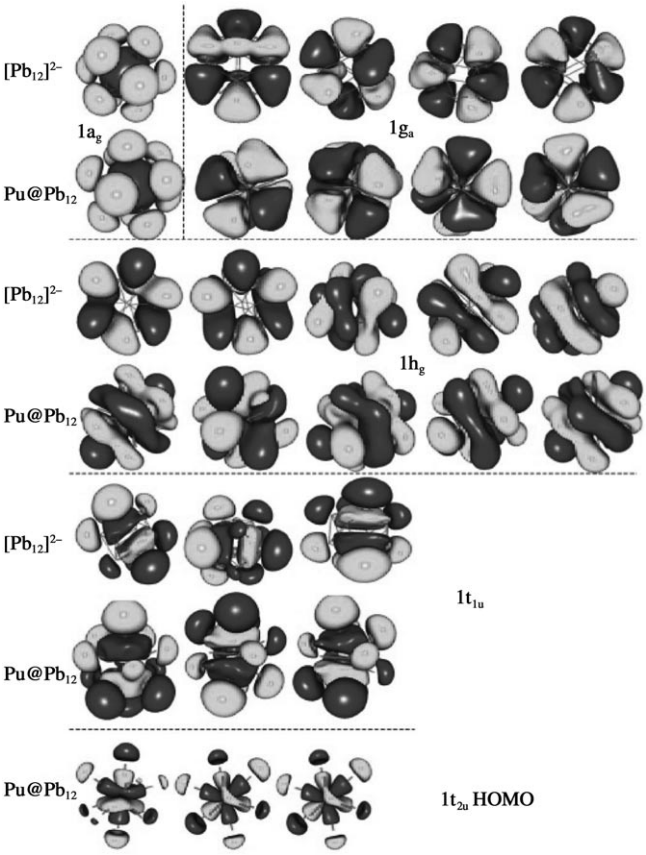

Figure 1. Comparison of valence molecular orbitals between the $[Pb_{12}]^{2-}$ and $Pu@Pb_{12}$ clusters.

Table 3: Bonding-energy (BE) analysis starting from the $[Pb_{12}]^{2-}$ and M^{x} fragments.[a]

Molecule[b]	BE [eV]	Pauli repulsion	Electrostatic	Steric	Orbital	6d	5f
$Yb@Pb_{12}$	−19.96	9.22	−18.12	−8.89	−11.07		
$[Th@Pb_{12}]^{4-}$	−4.49	61.13	−34.37	26.76	−31.25		
$[U@Pb_{12}]^{2-}$	−17.59	15.52	−12.11	3.41	−20.93		
$Pu@Pb_{12}$	−22.17	16.39	−21.54	−5.15	−17.02	−17.56	−20.17
$[Am@Pb_{12}]^{+}$	−39.18	15.91	−21.11	−11.20	−27.98	−28.03	−35.49
$[Cm@Pb_{12}]^{2+}$	−69.33	15.27	−33.25	−17.98	−51.36	−39.83	−52.86

[a] Pauli + electrostatic = steric; steric + orbital = BE. The last two columns give Dirac–Fock–Breit 6d and 5f orbital energies for the isolated actinide ion (see text). Note the relative descent of the latter. [b] Not performed on $[Np@Pb_{12}]^{-}$, which has an imaginary frequency.

For Yb and the later actinides Pu, Am, and Cm, the cluster symmetry remains icosahedral, as for empty plumbaspherene. No alternative minima were found. A slight radial expansion of the initial cage by up to 0.23 Å for the M–Pb distance is observed. On the contrary, compounds of early actinides, such as $[Th@Pb_{12}]^{4-}$, $[U@Pb_{12}]^{2-}$, and $[Np@Pb_{12}]^{-}$, are calculated to have a lower symmetry. A similar lowering of symmetry with elimination of the inversion symmetry was observed earlier by Straka et al.[16,17] for early f^0 actinide species of type AnO_2, AnO_4, AnF_6, AnF_8, and AnH_6. A possible explanation for this trend from a natural bond orbital analysis was a strong increase in the bonding contributions of 5f orbitals for Pu, Am, and Cm compounds, while the 6d character remained relatively unchanged.

The HOMO–LUMO gaps in Table 2 are rather large, especially for the Pu and Am compounds (1.93 and 2.45 eV, respectively). The bonding-energy decomposition for the $[M@Pb_{12}]^{x}$ clusters is given in Table 3. Owing to lower symmetry, longer Th–Pb distances, and strong 6d(Th) orbital hybridization, the behavior of the Th cluster stands apart from the others in having the lowest bonding energy of the series. Except for this compound, all the $[M@Pb_{12}]^{x}$ clusters studied are very stable, with absolute bonding energies larger than 15 eV with respect to the ionic dissociation limit. For comparison, a binding energy of −4.78 eV was reported for $Al@Pb_{12}$.[10] The electrostatic and Pauli repulsion terms follow the behavior of the interaction between the two charges. The global steric term (i.e., electrostatic plus Pauli repulsion) is minimal for the Pu cluster, and the most stable clusters correspond to an attractive steric term. For Pu, Am, and Cm clusters, that is, the icosahedral actinide compounds, the behavior of the orbital term follows that of the bonding-energy term. Moreover, the 6d and 5f orbital energies, also given in Table 3 for the isolated actinide ions, were obtained from numerical relativistic multiconfiguration Dirac–Fock calculations (MCDFGME

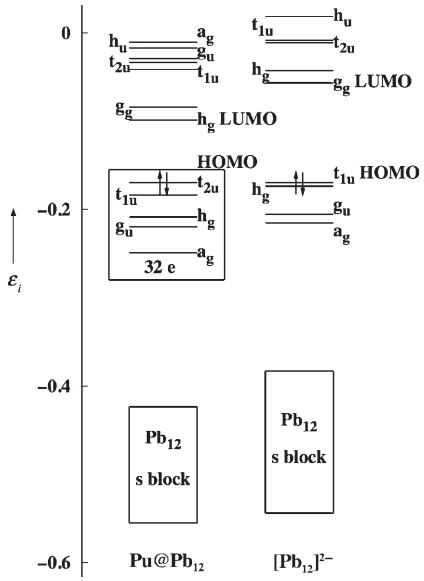

Figure 2. Orbital energies of $Pu@Pb_{12}$ and $[Pb_{12}]^{2-}$. The latter have been shifted to make the HOMOs equal.

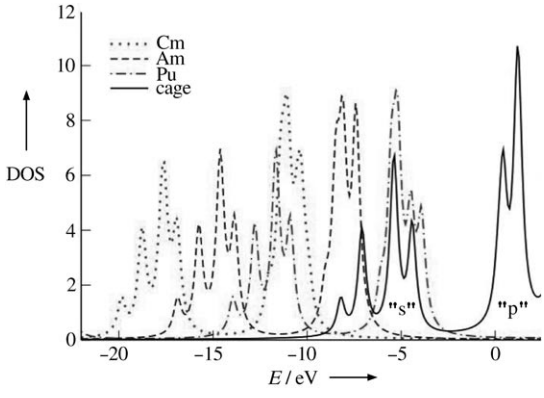

Figure 3. Density of states (DOS) for $[Pb_{12}]^{2-}$, $Pu@Pb_{12}$, $[Am@Pb_{12}]^{+}$, and $[Cm@Pb_{12}]^{2+}$ as a function of orbital energy; the respective Fermi energies are 1.3, −3.9, −6.2, and −9.9 eV.

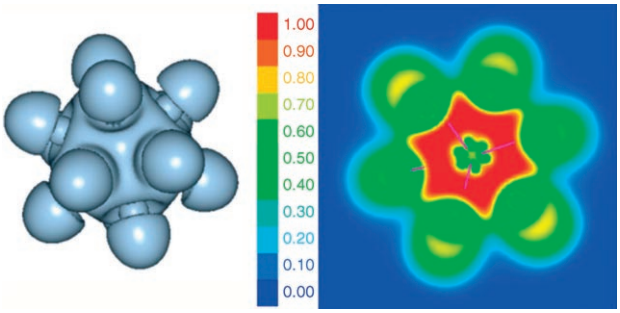

Figure 4. Isosurface (left) and cut-plane (right) ELF representations for $Pu@Pb_{12}$.

package[18]) including the contribution of the Breit interaction. For the Pu and Am clusters, the orbital term is determined by the 6d orbital energy, whereas that of the Cm cluster is controlled by the deep 5f orbital energy, consistent with a large bonding energy.

In Figure 1, the $Pu@Pb_{12}$ valence molecular orbitals can be compared with those of $[Pb_{12}]^{2-}$ with the same symmetry. The 16 molecular orbitals of the initial cage are present in addition to the three t_{2u} orbitals from the 5f orbitals of the plutonium atom (see Figure 2). One can see strong participation of the central-atom orbitals in the a_g, g_u, h_g, t_{1u}, and t_{2u} valence molecular orbitals, in order of increasing energy. Consequently, the Pu 7s, 7p, 6d, and 5f orbitals are involved in hybridization with the $[Pb_{12}]^{2-}$ cage orbitals. In our only lanthanide case, $Yb@Pb_{12}$, the energy spectrum is similar to those of An = Pu and An = Am. The 4f levels lie close to the top but do not strongly hybridize with the lead cage.

In $Pu@Pb_{12}$ the lowest vibrational frequencies (intrasphere motions of the central atom at about 28 cm^{-1}) are lower than the cage-deformation modes of the Pb_{12} cage. The latter range from 32 cm^{-1} for cage torsions to 107 cm^{-1} for Pu–Pb antisymmetric stretching.

These results enable us to conclude that this compound is the first example of a centered 32e system. For the $[Am@Pb_{12}]^{+}$ cluster, similar molecular orbitals were found but the energy order is different (see Figure S1 in the Supporting Information) because of stabilization of the 5f orbitals (see Table 3). This compound is our second example of the 32e principle. In the Pu/Am/Cm series, the energy of the valence molecular orbital decreases with a monotonous behavior, whereas the decrease of the t_{2u} orbitals is more pronounced. Consequently, the 5f orbitals in the $[Cm@Pb_{12}]^{2+}$ cluster are less hybridized because the 5f atomic orbitals are much deeper in energy (see Figure S1 in the Supporting Information). The Cm cluster does not fully correspond to a 32e system.

The electronic structure can further be gauged by calculating the density of states (DOS) and the ELF. Figure 3 shows the DOS of the Pu, Am, and Cm clusters and the $[Pb_{12}]^{2-}$ cage. A pronounced band structure can be observed for the cage corresponding to the "6s" and "6p" blocks of molecular orbitals. The band structure survives also for the endohedral compounds, but the DOS is shifted deeper in energy due to strong 5f(An)/6p(Pb) hybridization for An = Pu and An = Am. The strong 5f stabilization for Cm is clearly seen. The cage "s" and "p" bands, with a_g, g_u, h_g, and t_{1u} fine structure of the latter, are a smooth function of An, in contrast with the above-mentioned t_{2u} behavior. Figure 4 shows ELF representations of $Pu@Pb_{12}$ in volume and plane views. The isosurface shows nonnegligible deformation of the density around each Pb atom in the direction of the central Pu atom. More details are available from the cut-plane view of the ELF plot, which reveals a local electron maximum between the central Pu atom and the Pb atoms of the cage. The ELF representations of the Am cluster are quite similar to those for Pu. However, for the Cm cluster, the isosurface reveals a smaller contribution from the central atom, owing to weaker hybridization with the cage orbitals. It is known from the case of WAu_{12} that traditional forms of population analysis can fail abysmally.[19] A numerical study had to be performed. The population analysis must await further studies.

The spin–orbit splittings are discussed in the Supporting Information, and those found for g_u and h_g are very similar to the calculated value of Cui et al.[4] for the $[Pb_{12}]^{2-}$ cage. The

issue of modeling stiff, highly charged anions in solvents or crystals by free-ion calculations was discussed earlier.[20]. A solvent could also help to stabilize the ionic species.

In conclusion, our calculations suggest that the 26 6p electrons of $[Pb_{12}]^{2-}$ and the six 5f electrons of Pu^{2+} form a perfect, spdf-like 32-electron system. The future will show how general the concept is. Possible routes to form these clusters might be from a parent ion $[Pb_9]^{4-}$ in solution, or in the gas phase from laser-induced vaporization and subsequent mass spectrometry.

Received: October 13, 2006
Published online: January 16, 2007

Keywords: actinides · cluster compounds · density functional calculations · lead · ytterbium

[1] I. Langmuir, *Science* **1921**, *54*, 59 – 67, this paper mentions the 8-, 18-, and 32-electron closed shells and uses, on pp. 65–66, $[Fe(CO)_5]$, $[Ni(CO)_4]$, and $[Mo(CO)_6]$ as examples for 18e.
[2] P. Pyykkö, *J. Organomet. Chem.* **2006**, *691*, 4336 – 4340.
[3] P. Hrobárik, M. Straka, P. Pyykkö, *Chem. Phys. Lett.* **2006**, *431*, 6 – 12.
[4] L.-F. Cui, X. Huang, L.-M. Wang, J. Li, L.-S. Wang, *J. Phys. Chem. A* **2006**, *110*, 10169 – 10172.
[5] L.-F. Cui, X. Huang, L.-M. Wang, D. Zubarev, A. Boldyrev, J. Li, L.-S. Wang, *J. Am. Chem. Soc.* **2006**, *128*, 8390 – 8391.
[6] S. Neukermans, E. Janssens, Z. F. Chen, R. E. Silverans, P. v. R. Schleyer, P. Lievens, *Phys. Rev. Lett.* **2004**, *92*, 163401.
[7] X. Zhang, G. Li, X. Xing, X. Zhao, Z. Tang, Z. Gao, *Rapid Commun. Mass Spectrom.* **2001**, *15*, 2399 – 2403.
[8] E. N. Esenturk, J. Fettinger, Y.-F. Lam, B. Eichhorn, *Angew. Chem.* **2004**, *116*, 2184 – 2186; *Angew. Chem. Int. Ed.* **2004**, *43*, 2132 – 2134.
[9] E. Esenturk, J. Fettinger, B. Eichhorn, *J. Am. Chem. Soc.* **2006**, *128*, 9178 – 9186.
[10] D.-L. Chen, W. Q. Tian, W.-C. Lu, C.-C. Sun, *J. Chem. Phys.* **2006**, *124*, 154313, erratum: D.-L. Chen, W. Q. Tian, W.-C. Lu, C.-C. Sun, *J. Chem. Phys.* **2006**, *125*, 049901.
[11] C. Rajesh, C. Majumder, *Chem. Phys. Lett.* **2006**, *430*, 101 – 107.
[12] L.-F. Cui, X. Huang, L.-M. Wang, J. Li, L.-S. Wang, *Angew. Chem.* **2006**, DOI: 10.1002/ange.200603226; *Angew. Chem. Int. Ed.* **2006**, DOI: 10.1002/anie.200603226.
[13] A. Hirsch, Z. Chen, H. Jiao, *Angew. Chem.* **2000**, *112*, 4079 – 4081; *Angew. Chem. Int. Ed.* **2000**, *39*, 3915 – 3917.
[14] X. Gu, M. Ji, S. H. Wei, X. G. Gong, *Phys. Rev. B* **2004**, *70*, 205401.
[15] M. P. Johansson, D. Sundholm, J. Vaara, *Angew. Chem.* **2004**, *116*, 2732 – 2735; *Angew. Chem. Int. Ed.* **2004**, *43*, 2678 – 2681.
[16] M. Straka, K. G. Dyall, P. Pyykkö, *Theor. Chem. Acc.* **2001**, *106*, 393 – 403.
[17] M. Straka, P. Hrobárik, M. Kaupp, *J. Am. Chem. Soc.* **2005**, *127*, 2591 – 2599.
[18] J. Desclaux, P. Indelicato, MCDFGME 2005.10, 2005, http://dirac.spectro.jussieu.fr/mcdf/mcdf_code/mcdfgme_accueil.html.
[19] J. Autschbach, B. A. Hess, M. P. Johansson, J. Neugebauer, M. Patzschke, P. Pyykkö, M. Reiher, D. Sundholm, *Phys. Chem. Chem. Phys.* **2004**, *6*, 11 – 22.
[20] P. Pyykkö, Y.-F. Zhao, *J. Phys. Chem.* **1990**, *94*, 7753 – 7759.
[21] P. Pyykkö, N. Runeberg, *Angew. Chem.* **2002**, *114*, 2278 – 2280; *Angew. Chem. Int. Ed.* **2002**, *41*, 2174 – 2176.
[22] M. Walter, H. Häkkinen, *Phys. Chem. Chem. Phys.* **2006**, *8*, 5407 – 5411.

